DOI: 10.25092/baunfbed.342553 *J. BAUN Inst. Sci. Technol., 19(2), 264-274, (2017)*

Indium doping on the structural, surface and optical properties of CdS thin films prepared by ultrasonic spray pyrolysis method

Şilan BATURAY*

Physics Department, Science Faculty, Dicle University, Diyarbakir

Geliş Tarihi (Recived Date): 05.07.2017
Kabul Tarihi (Accepted Date): 05.10.2017

Abstract

CdS nanostructures are important and useful materials for photovoltaic applications. In this paper, pure CdS and In doped CdS (CdS:In) thin films were fabricated on soda lime glass substrate using ultrasonic spray pyrolysis (USP) method, to investigate the effect In concentration on the structural behavior, surface and optical properties of the CdS thin films by X-ray diffraction (XRD), Atomic Force Microscopy (AFM) and Ultraviolet–visible (Uv-vis) spectrophotometry. X-ray diffraction patterns of the pure and In doped CdS films indicated that pure CdS film had a mixed of cubic and hexagonal structure with polycrystalline nature while In doped CdS had a hexagonal structure with polycrystalline nature. Increasing the In doping ratio improve the (002) preferential orientation. The optical properties of the In-doped CdS and pure CdS films showed that the energy band gap of the In-doped CdS is a slightly lower than the energy band gap of the pure CdS film. The surface properties of the films showed that all thin films are compact and uniform.

Keywords: *CdS, Indium doping, Ultrasonic spray pyrolysis, structural properties*

Ultrasonik sprey piroliz yöntemiyle hazırlanan CdS ince filmlerin yapı, yüzey ve optik özelliklerine In katkısının etkisi

Özet

CdS nanoyapılar fotovoltaik uygulamalar için önemli ve yararlı malzemelerdir. Bu çalışmada, katkısız CdS ve In katkılı CdS (CdS: In) ince filmler ultrasonik sprey piroliz (USP) yöntemi kullanılarak cam alttaş üzerine büyütüldü ve X ışını kırınımı (XRD),

*Şilan BATURAY, silan@dicle.edu.tr, http://orcid.org/0000-0002-8122-6671
Ahmet TOMBAK, tahmet@yahoo.com, http://orcid.org/0000-0002-9997-1653

Atomik Kuvvet Mikroskopisi (AFM) ve spektrofotometri ile CdS ince filmlerin yapısal davranışları, yüzeyleri ve optik özellikleri üzerine konsantrasyonun etkisini araştırıldı. Saf ve In katkılı CdS filmlerin X-ışını kırınım desenleri, saf CdS filmin polikristal yapıya sahip bir kübik ve altıgenken, In katkılı CdS'nin polikristal yapılı altıgen bir yapıya sahip olduğunu görüldü. In katkılama oranının arttırılması tercihli yönelimi (002) artırdı. In-katkılı CdS ve saf CdS filmlerin optik özellikleri In-katkılı CdS'nin enerji bant aralığının saf CdS filmin enerji bant aralığından biraz daha düşük olduğunu görüldü. Filmlerin yüzey özelliklerinden tüm ince filmlerin kompakt ve düzgün olduğunu görülmektedir.

Anahtar Kelimeler: *CdS, İndiyum katkılama, Ultrasonik sprey piroliz, yapısal özellikler*

1. Introduction

In recent years, synthesis of semiconducting metal chalcogenide nanocrystals for applications studies have been attracted attention owing to the fact that they have different properties [1, 2]. Among of the metal chalcogenides, cadmium sulfide (CdS) is an important group II-VI semiconductors with a very important wide and direct band gap about 2.42 eV, high transparency, a small exciton Bohr radius of 2.5 nm and the high electron affinity [3]. In particular, CdS films with a wide range of forbidden energy are used as window material in solarcell [4]. Because of these properties of CdS, it is said that CdS is promising material for visible light absorption and one of the best candidate as window layer material in the thin film solar cells such as CdS/CdTe and ZnO/CdS/$CuInGaSe_2$ to get out of the recombination of photogenerated carriers, which increases the performance of the solar cells [5-7]. In addition, it can be used in many fields such as thermoelectric effect, quantum dots for various applications, luminescence, optoelectronic devices, photocatalytic hydrogen evolution, transistors and so on[8-13]. Many elements, like Zn [14-16], Ce [17], Mn [18], Cu [19], Ni [20], Fe [21] and In [22, 23] have been doped into CdS to demonstrate tunable optical and electrical properties.

Among the very different types of doped CdS films, the doped Cu could change the type of the semiconductor from *n* to *p* and acts as an acceptor in CdS semiconductor and also significantly enhances the conversion efficiency of thin film solar cells [24, 25]. However, the growth of In dopant with different dopant concentrations in films is demonstrated a tunable photoluminescent color from red to green that could improve the optoelectronic properties of CdS nanowires [24].

Various physical and chemical methods were used to fabricate the pure and doped CdS thin films. Rmili et al. fabricated Ni doped CdS thin film using spray pyrolysis [3]. Saravana et al. successfully prepared samarium into CdS nanocrystals by a simple co-precipitation method [26]. Thambidurai et al. prepared pure CdS and Co-doped CdS nanoparticles using a chemical precipitation method [27]. Orlianges et al. fabricated undoped CdS and carbon-doped CdS thin films by pulsed laser deposition (PLD) technique at low deposition temperature [28]. Hernandez-Como et al. achieved the maximum electron and hole concentrations up to 4×10^{18} cm^{-3} and 3×10^{20} cm^{-3} and low resistivity of 1Ω.cm and 0.2 Ω.cm for copper doped CdS and indium doped CdS thin films, respectively prepared by PLD [29].

Based on the literature, the influence of the deposition parameters such as flow rate and time of deposition on the ultrasonic spray pyrolysis deposited In doped CdS thin films not well investigated and also ultrasonic spray pyrolysis (USP) is a simple method to grow thin films that are uniform, homogenous, suitable for large area deposition and free from pinholes. Because of the aforementioned issues, in this report, the pure CdS and In doped CdS films were grown by USP and the effects of In on the structural, surface and optical properties of the CdS nanofilms were investigated according to increasing doping concentration.

2. Experimental details

The pure and CdS:In films were successfully fabricated on glass (soda-lime glass) using USP method an aqueous solution of 0.01M Cd [$C_4H_6CdO_4$, MW=266.53] and 0.01 M thiourea [CH_4N_2S, MW=76.12] as sources of Cadmium and sulphur ions, respectively. Indium chloride [($InCl_3$, MW=185.72] was used for In doping with different concentrations (1, 2, 3, and 5 at % In). The molar ratio of dopant ($InCl_3$) in the solution was varied from 0 to 5%. Substrate cleaning method is very important process in the fabrication of high quality thin films due to the fact that the contamination on the substrate surface causes low quality film growth and cracking. Therefore, the substrates were boiled firstly in a mixture of 5:1:1 H_2O, NH_3 and H_2O_2 for 20 min and then in 5:1:1 H_2O, HCL and H_2O_2 for 20 min. The obtained substrates were then ultrasonicated in acetone for 3 min. Prior to fabrication process, the substrates were again rinsed in deionised water for 5 min and dried under N_2 gas. The ultrasonic spray pyrolysis program (Sono Tek Exacta-Coat) was set to form a material gradient during spraying. The hot plate was set to constant 275 °C for 30 min to allow heat to distribution uniformly over the substrates. The precursor flow rate was set to 1ml/min and was carried by N_2 gas (41.3KPa) to substrate, which consisted of dry clean air. A fixed nozzle-substrate distance was kept at 9.5 cm and x-y directions speed was 15 mm/s to ensure homogenous, complete coverage. After this process, the fabricated films were annealed at 500 °C in tube furnace in air ambient under N_2 gas for 1 hour.

X-ray diffraction measurements were carried out with the help of Bruker Da Vinci Advanced-D8 (Cu Kα radiation, λ=1.5406 Å) with a 2θ = 25–75° at a scan rate of 1 °/min. Surface morphology of pure and In doped CdS films carried out using Park System XE 100 Atomic Force Microscopy (AFM). The optical transmittance and absorbance of the samples was measured in Shimadzu UV–3600 spectrophotometer.

3. Results and findings

3.1 Structural Studies

X-ray diffraction (XRD) pattern plays an important role for defining the orientations and crystallite size of the films. The typical XRD spectra of pure and In doped CdS nanofilms for different dopant ratio fabricated at 275 °C are shown in Fig.1. CdS films have four different crystalline orientations such as hexagonal, cubic (zinc blende) distorted rock salt and cubic rock salt [30]. Among these different crystalline structures, the most common and thermodynamically most stable phase is the hexagonal crystalline structure. CdS with cubic crystalline structure can be gained in nature is a metastable phase [31]. Another way, It can be said that at room temperature, the formation of cubic

CdS is thought over a metastable phase while the formation of hexagonal is the stable phase and thermal annealing may typically happen a phase transition from the formation of cubic phase to the formation of hexagonal phase [32]. The critical point for this phase transition is thought to be 300 °C [33]. The formation of rock salt coexists only under a hydrostatic pressure which ranged from 60 to 68 GPa [34]. Among these four crystal line structures, It can be seen that the pure CdS film shows the formation of different polymorphic phases of CdS (hexagonal and cubic) crystal structures, polycrystalline in nature, the crystallinity of the CdS films improves according to the different annealing temperature [23]. Xu et al. demonstrated that the major peaks in the XRD spectrum of the growth of different In-doped CdS can be well indexed to the formation of hexagonal CdS [23]. Kaur et al. Demonstrated that the uniform films with the formation of hexagonal or cubic phase or mixed hexagonal phase consist of the ion by ion process results [35]. For the sample annealed at 500 °C, the three strong reflections in the XRD pattern of pure CdS film show the crystalline nature with the diffraction angles 25.68°, 26.77° and 44.00° corresponding to (100), (002) and (110) planes of the mixed of hexagonal and cubic phase. For the In doped CdS, the three major diffraction peaks in the XRD pattern clearly show the multi crystalline nature corresponding to the diffraction angles around 25.50°, 26.66° and 44.00° corresponding to (100), (002) and (110) planes of hexagonal phase. The strong and broad peak for all films around 26.66° gives it is the preferred orientations along the (002) plane of hexagonal phase which also revealed the existence of better crystalline nature and it is suitable for photocatalytic reaction [36]. Megahid et al. demonstrated that the diffractogram includes one characterizing peak for the preferred orientations (0 0 2) plane of CdS film at 400 °C [37]. The FWHM (Full Width at Half Maximum) of the XRD peaks was slightly changing by the dopant ratio owing to variations in grain size. The *D* (grain size) was determined using the Debye–Scherrer equation [38]:

$$D = \frac{0.94\lambda}{\beta \cos\theta} \tag{1}$$

where λ is the wavelength of Cu Kα radiation (1.5406 Å), β is the angular peak full width at half maximum in radians along (100), (002) and (110) planes, and θ is the Bragg's diffraction angle. The calculated grain sizes of pure and In doped CdS are listed in table 1 and the grain size has changed with doping dopant.

The grain size of pure CdS and In doped CdS are changed from 26.5 to 660.6 Å. The grain size is increased from 82.0 to 226.5 Å by the addition of In from 0 to 5% for (002) preferential orientation. The highest value of the grain size is found to be 660.6 Å. for 3 at %. It can be said that the grain size tends to increase according as increasing In concentrations which may be attributed to the interference between In ions and CdS and In occupies the regular lattice site in CdS [39]. The higher grain size attributed to the better crystallinity of In doped CdS.

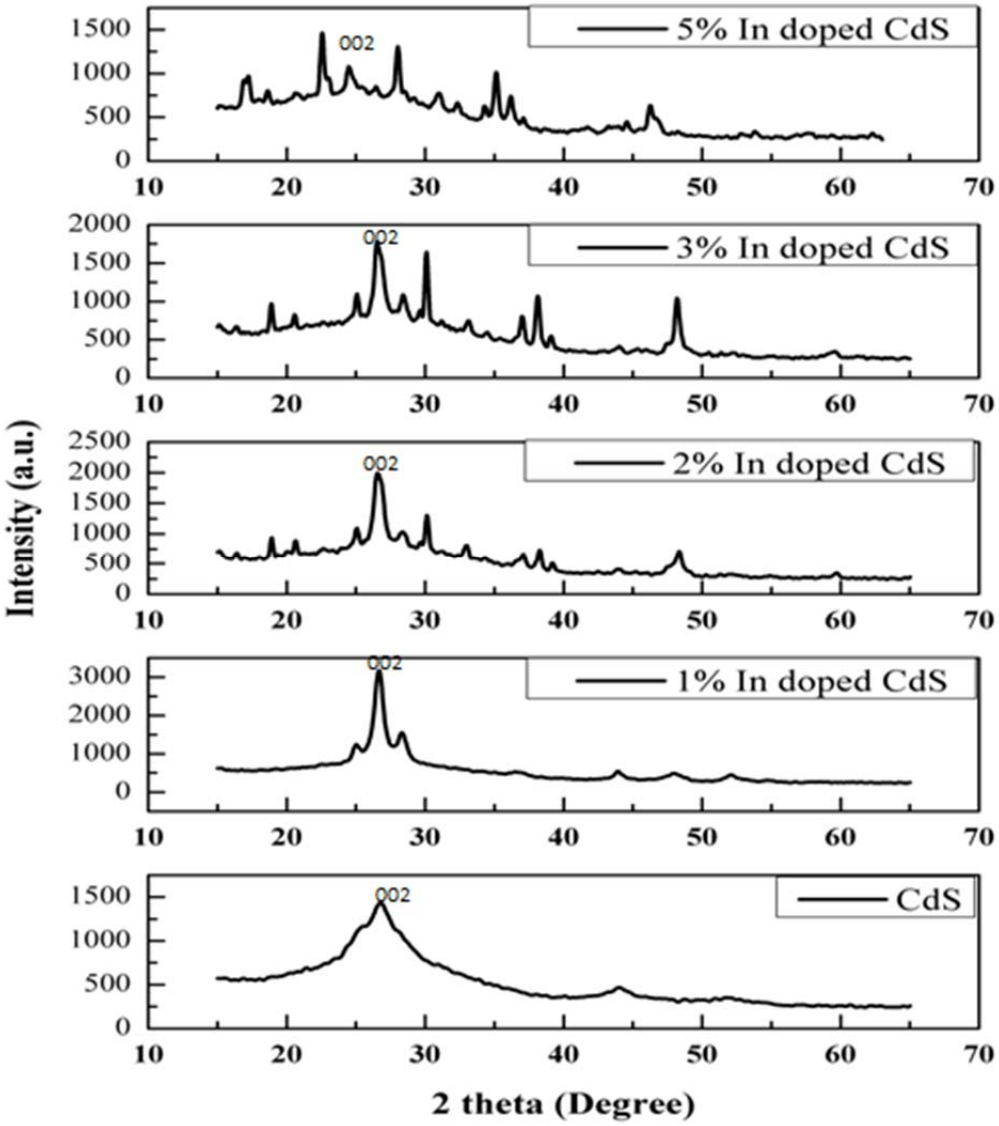

Figure 1. XRD pattern of pure and In doped CdS films

The micro-strain (ε) can be calculated using the formula:

$$(\varepsilon) = \frac{\beta \cos\theta}{4} \qquad (2)$$

It is also seen from Table 1 that the micro-strain is decreased by In doping for (100), (002) and (110) plane. The decrease of micro-strain causes the decrease the FWHM and the increase of grain size. Decreasing of the micro strain is increasing of lattice parameters and this decreasing of micro strain is attributed to the narrowing of diffraction peaks [40].

Table 1. XRD Patterns of pure and In doped CdS thin films grown by Ultrasonic Spray Pyrolysis (USP) for (a) 0 at%. (b) 1 at%. (c) 2 at%. (d) 3 at%. and (b) 5 at%.

Sample	2θ (degree)	d Interplanar distance (Å)	Relative Intensity (%)	FWHM (radians)	D Grain Size (Å)	ε Strain ($x10^{-3}$)	hkl (Orientation)
Pure CdS	25.68	3.47	58.0	0.056	26.5	13.6	100 (hexagonal)
	26.77	3.33	92.6	0.019	82.0	0.4	002 (hexagonal)
	44.00	2.06	13.8	0.017	86.7	3.9	110 (cubic)
1% In Doped CdS	25.07	3.55	18.9	0.006	237.8	6.0	100 (hexagonal)
	26.66	3.34	100	0.011	140.0	2.7	002 (hexagonal)
	43.93	2.06	7.80	0.009	187.6	2.1	110 (hexagonal)
2% In Doped CdS	25.07	3.55	27.6	0.005	117.4	1.2	100 (hexagonal)
	26.63	3.35	98.2	0.013	167.3	3.2	002 (hexagonal)
	43.96	2.30	9.30	0.009	166.3	2.1	110 (hexagonal)
3% In Doped CdS	25.07	3.55	34.1	0.004	367.1	1.0	100 (hexagonal)
	26.61	3.34	94.0	0.012	134.8	2.9	002 (hexagonal)
	44.00	2.30	13.3	0.003	489.5	0.7	110 (hexagonal)
5% In Doped CdS	24.60	3.62	97.4	0.003	660.6	0.7	100 (hexagonal)
	26.55	3.35	41.5	0.007	226.5	1.7	002 (hexagonal)

3.2 Surface properties

Morphologies of the pure and In doped CdS films deposited under USP method are shown in Fig 2(a-e) shows the AFM images in 5 μm × 5 μm scale and the corresponding 3D representations of all CdS films. From CdS images, we can see compact surface [41] and are not flat surfaces. The AFM images of all thin films demonstrate as fine 3D representations. It is said that the bright areas indicates the overgrown CdS crystallites of well-developed grain morphology. Then, the films were analyzed here possesses good morphologies and also may be used in various applications including catalysts and sensors.

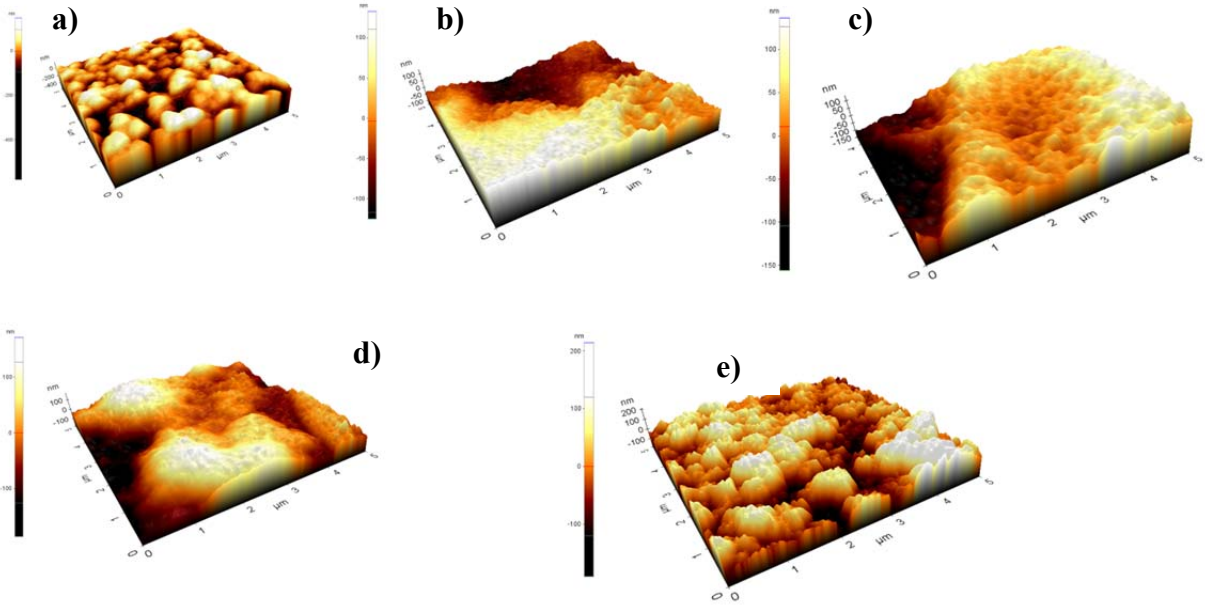

Figure 2. AFM images of a)Pure CdS b)1% In Doped CdS c) 2% In Doped CdS d) 3% In Doped CdS e) 5% In Doped CdS

The surface roughness of pure and In doped CdS (1, 2, 3 and 5 at % In) thin films is characterized by calculating the roughness parameters which are estimated by

examining the topography scans of all film's surface. The roughness values are found to be 48.41, 57.87, 58.74, 64.64 and 61.30 nm for pure, 1, 2, 3 and 5 at% In respectively. The root mean squares of the surface roughnesses of In doped CdS thin films deposited on soda lime glass substrate are increased as compared to pure CdS film. The roughness reaches its maximum value of 64.64 nm at 3 at % In-doping, then it decreases to 61.30 nm by increasing In to 5%. Apparently, CdS deposited on soda lime glass substrate is uniformity compact surface.

3.3 Optical properties

As is well known, exploration of optical properties, such as absorption and energy band gap is important for optoelectronic materials. Fig 3 gives the typical room temperature optical transmission spectra of all CdS films with various In concentrations pure, 1, 2, 3, and 5 at %. All the films indicate that the sharp optical absorption drop at the fundamental absorption band edge (λ ~500 nm) and the poor absorption nature of films which is attributed to electron excitation from the valence band to the conduction band. The noticed changes in the optical absorption are because of the different In dopant.

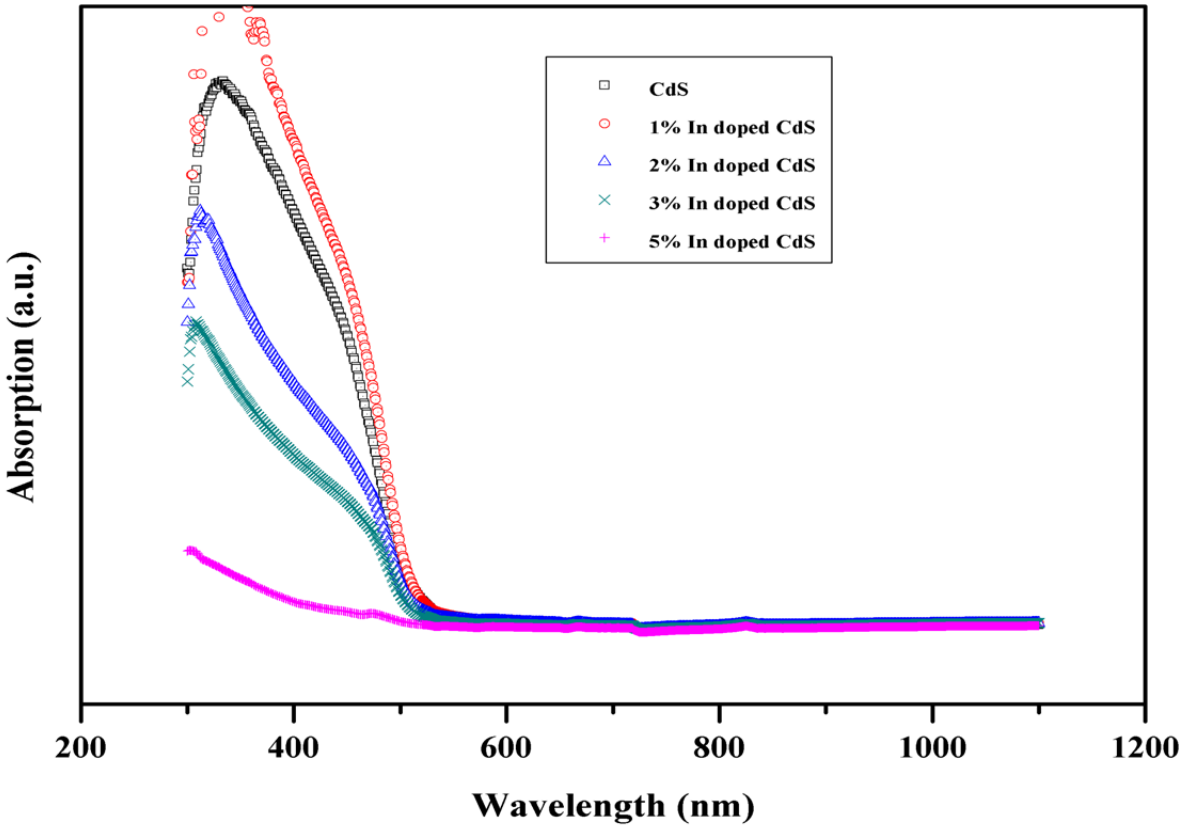

Figure 3. Absorption Spectra of Pure and In Doped CdS Films

For a crystalline semiconductor, it is known that the optical absorption coefficient α and the incident photon energy hv follows Eq. 3 [42]:

$$\alpha hv = A(hv - E_g)^n \quad (3)$$

where h, v, Eg, and A are Planck constant, light frequency, energy band gap value, and constant, respectively. While the exponent n is a constant that determines the type of optical transition and is 0.5 or 2 for direct or indirect band gap materials, respectively.

The energy band gap (*Eg*) of all films can be calculated from the data of UV–vis absorption spectra. The band energy gap of pure CdS was 2.53 eV, which is slightly bigger than 2.4 eV reported in literature [43]. The addition of In concentrations decreases the band gap from 2.53 to 2.47 eV for In = 0, 1, 2, 3, and 5 at %. The energy band gap decreased as the In concentration increased due to structural modifications. Another way, it may be said that the replacement of substitutional or interstitial Indium ions in the CdS lattice by In ions decreased the energy band of film. Consequently, decrease of the energy related to the direct transition because such In ions would lead to some additional energy levels in the CdS energy band gap close to the valence band edge.

4. Conclusion

Nanostructure pure and In-doped CdS films were grown successfully using ultrasonic spray pyrolysis (USP). The roughness of the pure CdS and In-doped CdS films were determined. The roughness values of films are ranged 48.41 to 64.64 nm for 0, 1, 2, 3, and 5 at % In, respectively. The root mean squares of the surface roughnesses of In doped CdS thin films are increased with increasing In dopant. AFM showed that the surface morphology and grain size of the CdS thin films was also influenced by the In dopant. XRD showed that the pure CdS thin films had a polycrystalline nature with mixed cubic and hexagonal phase while In doped CdS films show the formation of hexagonal phase with polycrystalline nature. The optical band gap of the In-doped CdS films slightly changed in the range 2.53–2.43 eV.

References

[1] Aldakov, D., Lefrançois A. and Reiss P., Ternary and quaternary metal chalcogenide nanocrystals: synthesis, properties and applications. **Journal of Materials Chemistry C**1, 24, 3756-3776, (2013).

[2] Yousefi, R., F. Jamali-Sheini and A.K. Zak. Metal chalcogenide hierarchical nanostructures for energy conversion devices. **Metal Chalcogenide Nanostructures for Renewable Energy Applications**, 189-232, (2014).

[3] Rmili, A., Ouachtari F., Bouaoud A., Louardi A., Chtouki T., Elidrissi B. and Erguig H., Structural, optical and electrical properties of Ni-doped CdS thin films prepared by spray pyrolysis. **Journal of Alloys and Compounds,** 557, 53-59, (2013).

[4] Karakaya, S., Gençyilmaz O. and Özbas Ö., In katkılı CdS filmlerinin optik, elektriksel ve yüzeysel özelliklerinin incelenmesi. **Balıkesir Üniversitesi Fen Bilimleri Enstitüsü Dergisi** ,14(2), 52-58, (2012).

[5] Graf, A., Maticiuc N., Spalatu N., Mikli V., Mere A., Gavrilov A. and Hiie J., Electrical characterization of annealed chemical-bath-deposited CdS films and their application in superstrate configuration CdTe/CdS solar cells. **Thin Solid Films**, 582, 351-355, (2015).

[6] Khosroabadi, S., Keshmiri S. and Marjani S., Design of a high efficiency CdS/CdTe solar cell with optimized step doping, film thickness, and carrier lifetime of the absorption layer. **Journal of the European Optical Society-Rapid publications,** 9, (2014).

[7] Yilmaz, S., Atasoy Y., Tomakin M. and Bacaksiz E., Comparative studies of CdS, CdS:Al, CdS:Na and CdS:(Al-Na) thin films prepared by spray pyrolysis. **Superlattices and Microstructures,** 88, 299-307, (2015).

[8] Eskandari, P., Kazemi F. and Azizian-Kalandaragh Y., Convenient preparation of CdS nanostructures as a highly efficient photocatalyst under blue led and solar light irradiation. **Separation and Purification Technology,** 120, 180-185, (2013).

[9] Li, G.-S., Zhang D.-Q. and Yu J.C., A New Visible-light photocatalyst: CdS quantum dots embedded mesoporous TiO2. **Environmental Science and Technology,** 43, 18, 7079-7085, (2009).

[10] Mahdi, M., Hassan J., Ahmed N.M., Ng S. and Hassan Z., Growth and Characterization of Cds single-crystalline micro-rod photodetector. **Superlattices and Microstructures,** 54, 137-145, (2013).

[11] Meng, J., Yu Z., Li Y. and Li Y., Pds-Modified Cds/Nis Composite as an efficient photocatalyst for H2 evolution in visible light. **Catalysis Today,** 225, 136-141, (2014).

[12] Wondmagegn, W., Mejia I., Salas-Villasenor A., Stiegler H., Quevedo-Lopez M., Pieper R. and Gnade B., Cds thin film transistor for inverter and operational amplifier circuit applications. **Microelectronic Engineering,** 157, 64-70, (2016).

[13] Zhang, Y., Zhang N., Tang Z.-R. and Xu Y.-J., Graphene transforms wide band gap ZnS to a visible light photocatalyst. The new role of graphene as a macromolecular photosensitizer. **ACS Nano,** 6, 11, 9777-9789, (2012).

[14] Baghchesara, M.A., Yousefi R., Cheraghizade M., Jamali-Sheini F. and Saáedi A., Photocurrent Application of Zn-Doped Cds Nanostructures Grown by Thermal Evaporation Method. **Ceramics International,** 42, 1, 1891-1896, (2016).

[15] Ma, L., Ai X.and Wu X., Effect of substrate and Zn doping on the structural, optical and electrical properties of CdSs thin films prepared by CBD method. **Journal of Alloys and Compounds,** 691, 399-406, (2017).

[16] Yang, X., Wang Z., Lv X., Wang Y. and Jia H., Enhanced photocatalytic activity of Zn-doped dendritic-like CdS structures synthesized by hydrothermal synthesis. **Journal of Photochemistry and Photobiology A: Chemistry,** 329, 175-181, (2016).

[17] Hurma, T. Effect of cerium incorporation on the structural and optical properties of Cds film. **Optik-International Journal for Light and Electron Optics,** 127, 22, 10670-10675, (2016).

[18] Nabi, A. The electronic and the magnetic properties of Mn doped wurtzite CdS: first-principles calculations. **Computational Materials Science,** 112, 210-218, (2016).

[19] Shaban, M., Mustafa M. and El Sayed A., Structural, optical, and photocatalytic properties of the spray deposited nanoporous CdS thin films; influence of copper doping, annealing, and deposition parameters. **Materials Science in Semiconductor Processing,** 56, 329-343, (2016).

[20] Darwish, M., Mohammadi A. and Assi N., Integration of nickel doping with loading on graphene for enhanced adsorptive and catalytic properties of CdS nanoparticles towards visible light degradation of some antibiotics. **Journal of Hazardous Materials,** 320, 304-314, (2016).

[21] Al-Zahrani, J., El-Hagary M. and El-Taher A., gamma irradiation induced effects on optical properties and single oscillator parameters of Fe-doped CdS

diluted magnetic semiconductors thin films. **Materials Science in Semiconductor Processing,** 39, 74-78, (2015).

[22] George, P., Sanchez A., Nair P. and Nair M., Doping of chemically deposited intrinsic CdS thin films to N type by thermal diffusion of indium. **Applied Physics Letters,** 66, 26, 3624-3626, (1995).

[23] Xu, J., Quan S., Zou Z., Guo P., Lu Y., Yan H. and Luo Y., Color-tunable photoluminescence from in-doped CdS nanowires. **Chemical Physics Letters,** 652, 216-219, (2016).

[24] Jie, J., Zhang W., Bello I., Lee C.-S. and Lee S.-T., One-dimensional Ii–Vi nanostructures: synthesis, properties and optoelectronic applications. **Nano Today,** 5, 4, 313-336, (2010).

[25] Poornima, K., Krishnan K.G., Lalitha B. and Raja M., CdS quantum dots sensitized Cu doped Zno nanostructured thin films for solar cell applications. **Superlattices and Microstructures,** 83, 147-156, (2015).

[26] Saravanan, L., Jayavel R., Pandurangan A., Jih-Hsin L. and Hsin-Yuan M., Influence of Sm doping on the microstructural properties of CdS nanocrystals. **Powder Technology,** 266, 407-411, (2014).

[27] Thambidurai, M., Muthukumarasamy N., Velauthapillai D., Agilan S. and Balasundaraprabhu R., Impedance spectroscopy and dielectric properties of cobalt doped CdS nanoparticles. **Powder Technology,** 217, 1-6, (2012).

[28] Orlianges, J.-C., Champeaux C., Dutheil P., Catherinot A. and Mejean T.M., Structural, electrical and optical properties of carbon-doped CdS thin films prepared by pulsed-laser deposition. **Thin Solid Films** ,519, 21, 7611-7614, (2011).

[29] Hernandez-Como, N., Berrellez-Reyes F., Mizquez-Corona R., Ramirez-Esquivel O., Mejia I. and Quevedo-Lopez M., CdS-based pin diodes using indium and copper doped CdS films by pulsed laser deposition. **Semiconductor science and technology,** 30, 6, 065003, (2015).

[30] Ziabari, A.A. and Ghodsi F., Growth, Characterization and studying of sol–gel derived CdS Nanoscrystalline thin films incorporated in polyethyleneglycol: effects of post-heat treatment. **Solar Energy Materials and Solar Cells,** 105, 249-262, (2012).

[31] Rittner, E.S. and Schulman J.H., Studies on the coprecipitation of cadmium and mercuric sulfides. **The Journal of Physical Chemistry,** 47, 8, 537-543, (1943).

[32] Khallaf, H., Chai G., Lupan O., Chow L., Park S. and Schulte A., Characterization of gallium-doped CdS thin films grown by chemical bath deposition. **Applied Surface Science,** 255, 7, 4129-4134, (2009).

[33] Zelaya-Angel, O., Alvarado-Gil J., Lozada-Morales R., Vargas H. and Ferreira da Silva A., Band-gap shift in CdS semiconductor by photoacoustic spectroscopy: evidence of a cubic to hexagonal lattice transition. **Applied Physics Letters,** 64, 3, 291-293, (1994).

[34] Suzuki, T., Yagi T., Akimoto S.I., Kawamura T., Toyoda S. and Endo S., Compression behavior of CdS and Bp up to 68 Gpa. **Journal of Applied Physics,** 54, 2, 748-751, (1983).

[35] Kaur, I., Pandya D.and Chopra K., Growth kinetics and polymorphism of chemically deposited CdS films. **Journal of The Electrochemical Society,** 127, 4, 943-948, (1980).

[36] Al-Douri, Y., Khasawneh Q., Kiwan S., Hashim U., Hamid S.A., Reshak A., Bouhemadou A., Ameri M. and Khenata R., Structural and optical insights to

enhance solar cell performance of CdS nanostructures. **Energy Conversion and Management,** 82, 238-243, (2014).

[37] Megahid, N., Wakkad M., Shokr E.K. and Abass N., Microstructure and electrical conductivity of in-doped CdS thin films. **Physica B: Condensed Matter** 353, 3, 150-163, (2004).

[38] Gupta, R., Ghosh K., Patel R., Mishra S. and Kahol P., Structural, optical and electrical properties of in doped CdO thin films for optoelectronic applications. **Materials Letters** 62, 19, 3373-3375, (2008).

[39] Muthusamy, M. and Muthukumaran S., Effect of Cu-doping on structural, optical and photoluminescence properties of CdS thin films. **Optik-International Journal for Light and Electron Optics,** 126, 24, 5200-5206, (2015).

[40] Pelleg, J. and Elish E., stress changes in chemical vapor deposition tungsten silicide (polycide) film measured by x-ray diffraction. **Journal of Vacuum Science and Technology A: Vacuum, Surfaces, and Films,** 20, 3, 754-761, (2002).

[41] Garcia, L., Loredo S., Shaji S., Martinez J.A., Avellaneda D., Roy T.D. and Krishnan B., Structure and properties of Cds thin films prepared by pulsed laser assisted chemical bath deposition. **Materials Research Bulletin,** 83, 459-467, (2016).

[42] Tauc, J., Absorption edge and internal electric fields in amorphous semiconductors. **Materials Research Bulletin,** 5, 8, 721-729, (1970).

[43] Weller, H., Colloidal semiconductor q-particles: chemistry in the transition region between solid state and molecules. **Angewandte Chemie International Edition in English,** 32, 1, 41-53, (1993).